Articles

Identification of Binding Sites for Both dsRBMs of PKR on Kinase-Activating and Kinase-Inhibiting RNA Ligands†

Richard J. Spanggord, Momchilo Vuyisich, and Peter A. Beal*

Department of Chemistry, University of Utah, Salt Lake City, Utah 84112

Received November 15, 2001; Revised Manuscript Received December 26, 2001

ABSTRACT: The RNA-dependent protein kinase (PKR) is an interferon-induced, RNA-activated enzyme that phosphorylates and inhibits the function of the translation initiation factor eIF-2. PKR has a double-stranded RNA-binding domain (dsRBD) composed of two copies of the dsRNA binding motif (dsRBM). PKR's dsRBD is involved in the regulation of the enzyme as dsRNAs of cellular and viral origins bind to the dsRBD, leading to either activation or inhibition of PKR's kinase activity. In this study, we site-specifically modified each of the dsRBMs of PKR's dsRBD with the hydroxyl radical generator EDTA·Fe and performed cleavage studies on kinase-activating and kinase-inhibiting RNAs. These experiments led to the identification of binding sites for the individual dsRBMs on various RNA ligands including a viral activating RNA (TAR from HIV-1), a viral inhibiting RNA (VA_I RNA from adenovirus), an aptamer RNA that activates PKR, and a small synthetic inhibiting RNA. These results indicate that some RNAs interact only with one dsRBM, while others can bind both dsRBMs of PKR. In addition, EDTA·Fe modification coupled with site-directed mutagenesis was used to assess the extent of cooperativity in the binding of the two dsRBMs. These experiments support the hypothesis that simultaneous binding of both dsRBMs of PKR occurs on kinase activating RNA ligands.

The RNA-dependent protein kinase (PKR)[1] is an interferon-inducible enzyme that contributes to the cessation of cell growth in response to viral infection (*1*). In vitro, PKR is activated by binding to RNA molecules with extensive duplex secondary structure (*2*). In vivo, the enzyme is believed to be activated by viral double-stranded RNA (dsRNA) or viral replicative intermediates comprising dsRNA (*3*). Activated PKR phosphorylates the alpha subunit of the heterotrimeric eukaryotic translation initiation factor 2 (eIF2α) (*4*). Phosphorylation of eIF2α inhibits initiation of protein synthesis by the eIF2 complex (*5*). Viruses that infect eukaryotic cells circumvent the activity of this antiviral kinase in a variety of ways. Some, such as adenovirus and Epstein Barr virus, synthesize highly structured RNAs that bind PKR and block activation (VA and EBER RNAs, respectively) (*6, 7*).

Human PKR is 68 kDa with an approximately 20 kDa N-terminal double-stranded RNA-binding domain (dsRBD) and a C-terminal protein kinase domain (*8*). The dsRBD is composed of two copies of the dsRNA-binding motif (dsRBM I, dsRBM II), a sequence motif found in many dsRNA-binding proteins (Figure 1) (*9*). These proteins bind dsRNA in a largely sequence-independent fashion and are involved in a myriad of biological processes such as RNA editing (*10*), RNA trafficking (*11*), RNA processing (*12*), transcriptional (*13*), and translational regulation (*14*). The solution structure of the 20 kDa PKR dsRBD was determined by NMR spectroscopy demonstrating that both dsRBMs have the characteristic α−*β*−*β*−*β*−α fold, which has been observed with several other dsRBMs (Figure 1) (*15*). Although proteins with these motifs have been shown to be involved in many different processes in the cell, little information is available about how proteins with multiple copies of dsRBMs recognize their RNA ligands. Reports of

† This work was supported by a grant from the National Institutes of Health to P.A.B. (GM-57214).

* To whom correspondence should be addressed. Tel: 801-585-9719. Fax: 801-581-8433. E-mail: beal@chemistry.utah.edu.

[1] Abbreviations: PKR, RNA-dependent protein kinase; eIF2α, alpha subunit of eukaryotic initiation factor 2; dsRBD, double-stranded RNA binding domain; bp, base pair; nt, nucleotide; dsRBM, double-stranded RNA binding motif; EDTA, ethylenediamine tetraacetic acid; Tris, tris-(hydroxymethyl)aminomethane; DTT, dithiothreitol; E29C-EDTA·Fe, GSEE (human PKR 1−184) bearing the E29C, C121V, and C135V mutations modified with bromoacetamidobenzyl-EDTA·Fe at position 29; D38C-EDTA·Fe, GSEE (human PKR 1−184) bearing the D38C, C121V, and C135V mutations modified with bromoacetamidobenzyl-EDTA·Fe at position 38; Q120C-EDTA·Fe, GSEE (human PKR 1−184) bearing the Q120C, C121V, and C135V mutations modified with bromoacetamidobenzyl-EDTA·Fe at position 120; K150A, E29C-EDTA·Fe, GSEE (human PKR 1−184) bearing the E29C, K150A, C121V, and C135V mutations modified with bromoacetamidobenzyl-EDTA·Fe at position 29; K60A, Q120C-EDTA·Fe, GSEE (human PKR 1−184) bearing the K60A, Q120C, C121V, and C135V mutations modified with bromoacetamidobenzyl-EDTA·Fe at position 120; TAR RNA, transactivating response element RNA from HIV-1; VA_I RNA, adenoviral PKR inhibiting RNA I; EBER RNA, Epstein−Barr virus-encoded RNA; DMSO, dimethyl sulfoxide; TBE, 90 mM Tris, 90 mM boric acid, 2 mM EDTA; SELEX, systematic evolution of ligands by exponential enrichment; PMSF, phenylmethylsulfonyl fluoride; Hepes, *N*-(2-hydroxyethyl)piperazine-*N*′-(2-ethanesulfonic acid).

10.1021/bi0120594 CCC: $22.00
Published on Web 03/15/2002

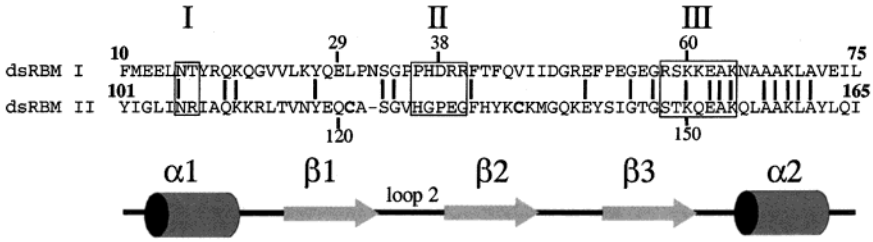

FIGURE 1: (Top) Amino acid sequence of dsRBMs I and II that make up human PKR's dsRBD. Amino acid positions where cysteine was incorporated are highlighted, and the two natural cysteines mutated to valine are bolded. Also highlighted are the RNA-binding residues K60 in dsRBM I and K150 in dsRBM II (*34*). Boxed are the three clusters of surface amino acids corresponding to regions I, II, and III shown to be in contact with RNA in the crystal structure of dsRBM II of Xlrbpa in complex with dsRNA (*16*). (Bottom) Location of secondary structural elements (α helices, *β* strands, and loop 2) in the sequence of PKR's dsRBMs (*15*).

high-resolution structures only describe the binding of single dsRBMs to their RNA ligands with no structures available for multi-dsRBM containing proteins in complex with RNA. In the crystal structure of dsRBM II from the *Xenopus laevis* protein Xlrbpa bound to duplex RNA, the protein contacts a 16-bp RNA duplex in one major groove and two adjacent minor grooves using three different clusters of surface amino acids (regions I, II, and III) (*16*). The crystal structure clearly explains the selectivity for dsRNA over dsDNA due to the multiple protein contacts made with the 2′-hydroxyl groups. The lack of numerous direct amino acid contacts made with specific RNA bases also explains the observed absence of a base-sequence requirement in the dsRBM RNA-binding. In the NMR structure of the dsRBM III from *Drosophila* protein Staufen bound to a stem-loop RNA, the single-stranded RNA loop is bound by the N-terminal alpha-helix (α1) of the dsRBM, demonstrating the versatility of RNA binding by the dsRBM (*17*). In our previous work, we showed that dsRBM I of PKR's dsRBD can bind to synthetic and viral RNA ligands selectively and in a specific orientation (*18*).

The dsRBMs play a key role in PKR regulation as both kinase-activating and inhibiting RNAs bind PKR via these motifs. Previous studies of PKR's dsRBD have provided some insight into how the two dsRBMs interact with RNA ligands. It has been shown that dsRBM I has a higher affinity for dsRNA than does dsRBM II (*19*). However, both motifs are required for maximal dsRNA binding by PKR's dsRBD, suggesting cooperativity between the two motifs (*20*, *21*). Furthermore, binding of RNA to PKR's dsRBD induces an activating conformational change in the kinase domain of the enzyme (*2*, *22*, *23*). Recent biochemical and biophysical studies led to the suggestion that dsRBM II of PKR is an autoinhibitory domain, masking the kinase domain in the inactive conformation (*24*, *25*). The authors suggest that an RNA ligand of PKR capable of kinase activation can bind cooperatively to both dsRBMs, relieving the kinase domain of its interaction with dsRBM II, leading to kinase activation and autophosphorylation (*25*). A corollary of this hypothesis states that an inhibiting RNA ligand interacts with PKR in a distinct manner that does not allow for relief of autoinhibition by dsRBM II. Interestingly, although only 16−18 bp of duplex RNA are required for binding to PKR, activation of the enzyme requires a longer duplex region (*2*, *20*). This is consistent with the hypothesis that an activation event requires the simultaneous binding of both dsRBMs.

To test ideas about the differences between complexes formed between PKR and kinase-activating and kinase-inhibiting RNAs, experiments that identify the location of PKR's dsRBMs in complexes with both activating and inhibiting ligands are required. High-resolution structural analysis of various RNA complexes of PKR is complicated by the relatively low binding selectivity associated with the protein, potentially leading to mixtures of PKR−RNA complexes. However, using affinity cleaving with EDTA·Fe-modified proteins, we can rapidly identify binding sites on an RNA ligand for the individual dsRBMs of PKR. We previously demonstrated that the dsRBD of PKR (amino acids 1−184) could be modified with EDTA·Fe at either Glu 29 or Asp 38 in dsRBM I and the resulting protein-EDTA·Fe conjugates selectively cleaved RNA ligands of PKR (*18*). The binding site and orientation of dsRBM I were inferred from the cleavage pattern on each RNA ligand. In addition, by combining the cleavage analysis with mutagenesis of the protein and/or the RNA ligand, we can probe the cooperativity in the binding of the two dsRBMs to a given RNA structure.

Using this approach, we investigated the binding of PKR's dsRBD to a viral activating RNA (TAR from HIV-1), a viral inhibiting RNA (VA_I RNA from adenovirus), an aptamer RNA that activates PKR, and a small synthetic inhibiting RNA. For the two activating RNAs studied, binding sites for both dsRBM I and dsRBM II were identified that could support simultaneous binding of these two motifs. The aptamer RNA appears to bind dsRBM I in two distinct ways, only one of which involves simultaneous binding of both motifs. This result emphasizes the potential complexity of interactions between PKR and various RNA ligands. The small, synthetic inhibitor only binds dsRBM I, whereas the inhibiting VA_I RNA has a single major binding site that can be occupied by either dsRBM I or dsRBM II. Thus, the results of these experiments are consistent with the hypothesis that simultaneous binding of both dsRBMs of PKR occurs on kinase-activating RNA ligands. In addition, RNAs that cannot simultaneously bind both motifs function as antagonists of kinase activation.

MATERIALS AND METHODS

General. Distilled, deionized water was used for all aqueous reactions and dilutions. Biochemical reagents were obtained from Sigma/Aldrich unless otherwise noted. Restriction enzymes and nucleic acid modifying enzymes were purchased from Pharmacia, Boehringer-Mannheim or New England Biolabs. Oligonucleotides were prepared on a Perkin-Elmer/ABI model 392 DNA/RNA synthesizer with *β*-cyanoethyl phosphoramidites. 5′-Dimethoxytrityl protected 2′-deoxyadenosine, 2′-deoxyguanosine, 2′-deoxycytidine, and

thymidine phosphoramidites were purchased from Perkin-Elmer/ABI. 5′-Dimethoxytrityl-2′-*tert*-butyldimethylsilyl protected adenosine, guanosine, cytidine, and uridine phosphoramidites were purchased from Glen Research. [γ-^{32}P] ATP (6000 Ci/mmol) was obtained from Dupont NEN. Storage phosphor autoradiography was carried out using imaging plates purchased from Kodak. A Molecular Dynamics STORM 840 was used to obtain all data from phosphor imaging plates. Bromoacetamidobenzyl-EDTA·Fe was purchased from Dojindo Laboratories. Molecular modeling was performed on a Silicon Graphics O_2 work station running Insight II (Biosym).

Construction of the PKR-dsRBD Single Cysteine Mutants. As described previously, mutants of human PKR dsRBD (amino acids 1−184) were obtained as glutathione-*S*-transferase (GST) fusion proteins by expression in *Escherichia coli* using the bacterial expression plasmid pGEX-2T (Pharmacia) (*26*). An expression plasmid for the cysteine-free PKR dsRBD was constructed as previously described (*26*). The cysteines found naturally in dsRBM II were previously shown not to be essential in the RNA binding or kinase activation of PKR (*26*). The E29C and D38C single cysteine mutants were constructed by PCR mutagenesis as previously described (*18*). All other PKR dsRBD mutants described in this work were constructed by Quick Change site-directed mutagenesis (Stratagene). To probe the location of dsRBM II in complexes with RNA, we identified an amino acid in dsRBM II in the position analogous to that of E29 (Q120) by sequence alignment (Figure 1) (*9*). A cysteine mutation was introduced at this position, and the resulting protein was alkylated to generate the PKR dsRBD Q120C-EDTA·Fe conjugate. This conjugate was shown to bind RNA with an affinity similar to that of wild-type PKR dsRBD using gel mobility shift assays with various PKR ligands (data not shown). The following primers were used for mutagenesis of the PKR dsRBD: Q120C (mutagenic oligos): 5′-ACTGTAAATTATGAATGTgtaGCATCGGGGGTG-3′; 5′-CACCCCCGATGCtacACATTCATAATTTACAGT-3′; K150A (mutagenic oligos): 5′-ATTGGTACAGGTTCTACT-GCCCAGGAAGCAAAACAATTG-3′; 5′-GGCCAATTG-TTTTGCTTCCTGGGCAGTAGAACCTGTACCAAT-3′. K60A (mutagenic oligos): 5′-GAAGGTGAAGGTAGAT-CAGCCAAGGCAAAAAATGCC-3′;5′-GGCATTTTTTGCT-TCCTTGGCTGATCTACCTTCACCTTC-3′. Lower case nucleotides represent the retention of the valine 121 mutation, and underlined nucleotides represent introduced mutations. All single mutations were verified by DNA sequencing.

Expression and Purification of PKR dsRBD Proteins. PKR dsRBD expression was performed as previously described (*26*). Briefly, BL-21 *E. coli* expressed GST fusion PKR dsRBD was incubated with glutathione sepharose that was prewashed in glutathione sepharose buffer (20 mM TrisHCl, pH = 8.3, 1 mM DTT, 1 mM PMSF) for 4 h at 4 °C. Unbound proteins were removed by successive washes with glutathione sepharose buffer supplemented with 200 mM NaCl and thrombin buffer [120 mM TrisHCl (pH = 8.6), 150 mM NaCl, 7 mM $CaCl_2$]. The GST domain was removed by incubating fusion protein with 40 units of thrombin for 12 h at 4 °C, and the reaction was quenched with the addition of PMSF (1 mM final concentration). After dialysis, the PKR dsRBD was aliquoted into 20−30 μL fractions and stored at −20 °C (*26*).

Preparation of RNA Ligands of PKR. Generation of the synthetic stem−loop ligand of PKR was performed on a Perkin-Elmer DNA/RNA synthesizer as previously described (*18*). VA_I RNA and the 92 nt aptamer were generated by transcription with T7 RNA polymerase as previously described (*18*, *26*). The nucleotides of VA_I RNA underlined in Figure 8 represent sequence changes made to facilitate cloning. This region of VA_I RNA is outside the previously described PKR binding site (*27*). TAR RNA was generated by transcription with T7 RNA polymerase (*28*). Generation of the necessary DNA transcription template and T7 promoter (5′-TAATACGACTCACTATAG-3′) was performed via automated DNA synthesis. Transcription of TAR RNA was performed by mixing 100 pmol of template strand with 120 pmol of the 18 mer T7 promoter with transcription buffer [40 mM TrisHCl (pH = 7.4), 14 mM $MgCl_2$, 2 mM spermidine, 1 mM DTT, 1 u/μL RNasin, and 4 mM each NTP] in a 100 μL reaction volume. TAR transcripts were purified on a 19% denaturing gel and extracted as previously described (*26*).

Bromoacetamidobenzyl-EDTA·Fe Modification of Single Cysteine PKR dsRBD Mutants. Conjugation of the PKR dsRBD cysteine mutants with the nucleic acid cleaving reagent bromoacetamidobenzyl-EDTA·Fe was performed as previously described (*18*). Briefly, a 1 mL solution of 100−250 μM PKR dsRBD cysteine mutant was incubated with 1 mM DTT for 12 h at 4 °C. The solution was dialyzed into degassed modification buffer [10 mM Hepes (pH = 8.0), 0.1 M NaCl, 5% glycerol, and 0.1 mM EDTA] until all DTT had been removed (3 h). The PKR dsRBD (325 μL solution) was mixed with 11.5 μL of a 26 mM solution of bromoacetamidobenzyl-EDTA·Fe (in DMSO, 1 mM final concentration) followed by a 3 h incubation at 37 °C. Conjugation reactions were quenched by the removal of excess reagent via immediate dialysis into storage buffer [25 mM TrisHCl (pH = 7.0), 10 mM NaCl] in the dark at 4 °C. Bromoacetamidobenzyl-EDTA·Fe modified proteins were stored at −20 °C and the extent of PKR dsRBD modification was analyzed via electrospray ionization mass spectrometry as previously described (*18*). The masses observed indicated that the EDTA ligand of each protein conjugate was bound to Fe, and no additional Fe was used for the cleavage experiments.

Affinity Cleavage Experiments. RNA complexes with PKR dsRBD modified with bromoacetamidobenzyl-EDTA·Fe were formed by incubating 4 μM protein (unless otherwise noted) with 5′- and 3′-end labeled RNA at room temperature for 7 min in 25 mM TrisHCl (pH = 7.0), and 10 mM NaCl. Protein−RNA complexes were analyzed via gel mobility shift assays as previously described (*26*). PKR dsRBD·RNA complexes (20 μL final reaction volume) were probed by initiating hydroxyl radical formation with the addition of cleavage reagents [0.01% H_2O_2 (0.001% H_2O_2 with TAR RNA) and 5 mM sodium ascorbate] followed by incubating at room temperature for five minutes. To ensure that the cleavage observed came from reaction of the protein-EDTA·Fe conjugate, a control experiment was performed with each RNA and 4 μM each of free EDTA, $Fe(NH_4)_2(SO_4)_2 \cdot 6H_2O$, and unmodified dsRBD cysteine mutant. Reactions were quenched by the addition of 80 μL of distilled water followed by phenol/chloroform extraction and ethanol precipitation. Cleaved RNA was resuspended into 7 μL of loading dye

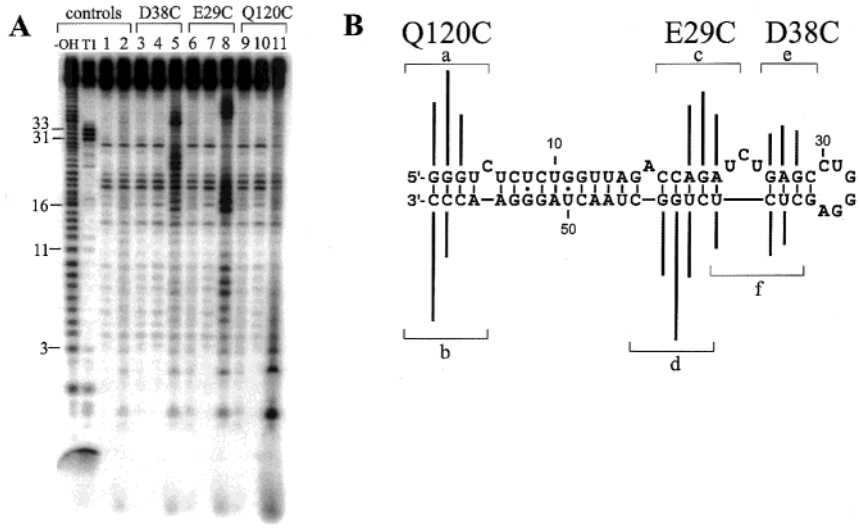

FIGURE 2: Affinity cleaving of TAR RNA using the EDTA·Fe modified PKR dsRBD. (A) Storage phosphor autoradiogram of a 19% denaturing polyacrylamide gel separating the 5′-end labeled RNA cleavage products. -OH: alkaline ladder; T1: RNase T1 (G ladder); lane 1: RNA only; lane 2: RNA in the presence of free EDTA·Fe and cleavage reagents (see Materials and Methods for details); lane 3: unmodified D38C and RNA in the presence of free EDTA·Fe and cleavage reagents; lane 4: D38C-EDTA·Fe and RNA; lane 5: D38C-EDTA·Fe and RNA in the presence of cleavage reagents; lane 6: unmodified E29C and RNA in the presence of free EDTA·Fe and cleavage reagents; lane 7: E29C-EDTA·Fe and RNA; lane 8: E29C-EDTA·Fe and RNA in the presence of cleavage reagents; lane 9: unmodified Q120C and RNA in the presence of free EDTA·Fe and cleavage reagents; lane 10: Q120C-EDTA·Fe and RNA; lane 11: Q120C-EDTA·Fe and RNA in the presence of cleavage reagents. (B) The Q120C (brackets a and b), E29C (brackets c and d), and D38C (brackets e and f) major cleavage sites are mapped onto TAR RNA's secondary structure where line lengths indicate relative cleavage efficiencies (*30*). To obtain cleavage data at the 3′-end of the TAR molecule, it was 3′-end labeled prior to the cleavage reaction (data not shown).

(96% formamide in 0.2× TBE with xylene cyanol dye) and analyzed via denaturing polyacrylamide gel electrophoresis. Data were obtained from the gels using storage phosphor autoradiography and a STORM PhosphorImager (Molecular Dynamics). Mapping of the cleavage data was performed as previously described (*18*). All cleavage sites mapped were confirmed with 3′-end labeled RNA and no major cleavage sites other than those mapped were observed (data not shown).

Molecular Modeling. A model of TAR RNA bound by the PKR dsRBD was generated using Insight II (Biosym) on a Silicon Graphics O2 workstation. The NMR structure of TAR RNA (nucleotides 19−43) was obtained from the Protein Data Bank (1ANR) (*29*). The rest of TAR RNA (nucleotides 1−18 and 44−59) was built using the biopolymer module and minimized using Discover 3 in Insight II. Both dsRBMs of PKR's dsRBD shown were generated using the crystal structure coordinates reported for Xlrbpa's dsRBM II (*16*). Both dsRBMs of PKR have been shown by NMR spectroscopy to have the characteristic α−β−β−β−α topology observed for dsRBM II of Xlrbpa (*15*). The E29 and Q120 amino acid positions of PKR's dsRBM I and dsRBM II were mapped onto the ribbon structure of the Xlrbpa dsRBM II using the analogous V133 amino acid position and the homology modeling module in Insight II (*9*). The D38 amino acid position of PKR's dsRBM I was also mapped using the analogous K142 amino acid position of Xlrbpa dsRBM II. Docking of both dsRBMs was carried out manually in Insight II maintaining the locations of the three regions of RNA contact observed in the Xlrbpa dsRBM II·RNA structure and guided by the cleavage data obtained in this work. The 22-amino acid linker was built and ligated onto both motifs and minimized using Discover 3 to generate the completed model (*8*).

RESULTS

Binding Sites of dsRBM I and dsRBM II of PKR's dsRBD on TAR RNA from HIV-1. The transactivating response element (TAR) RNA from HIV-1 is a 59 nt RNA that forms a stem−loop structure with a 24 bp duplex region interrupted by three bulges (*30*). This RNA has been shown by others to be an activator of PKR's kinase domain at low concentrations and to inhibit the enzyme at higher concentrations (*31*, *32*). When the dsRBD of PKR is modified with EDTA·Fe at position 38 in loop 2 of dsRBM I, TAR is cleaved in the complex at nucleotides in the base-paired region near the loop of the stem−loop structure (Figure 2A, lane 5 and Figure 2B). With position 29 modified with EDTA·Fe, the nucleotides approximately 4 bp further away from the loop are cleaved (Figure 2A, lane 8 and Figure 2B). The relative positions of the cleavage patterns generated by these two EDTA·Fe conjugates are similar to those observed with other stem−loop RNAs (*18*). These results indicate that dsRBM I of PKR's dsRBD binds near the RNA loop in an orientation placing loop 2 of dsRBM I near the RNA loop. The Q120C-EDTA·Fe conjugate cleaved the nucleotides residing at the very end of the TAR RNA duplex (Figure 2A, lane 11 and Figure 2B). This places dsRBM II at the 3′- and 5′-end of TAR and indicates that dsRBM II has a separate binding site on the RNA at the end opposite that of dsRBM I. As observed with dsRBM I, dsRBM II binds this RNA selectively with no other observed cleavage sites.

The Binding Sites for dsRBM I and dsRBM II of PKR's dsRBD on a Kinase-Activating Aptamer. We next investigated a 92 nt activating RNA ligand discovered during SELEX experiments (aptamer) (*33*). Secondary structure predictions along with chemical probing experiments indicated that this RNA folds into a structure with two stem

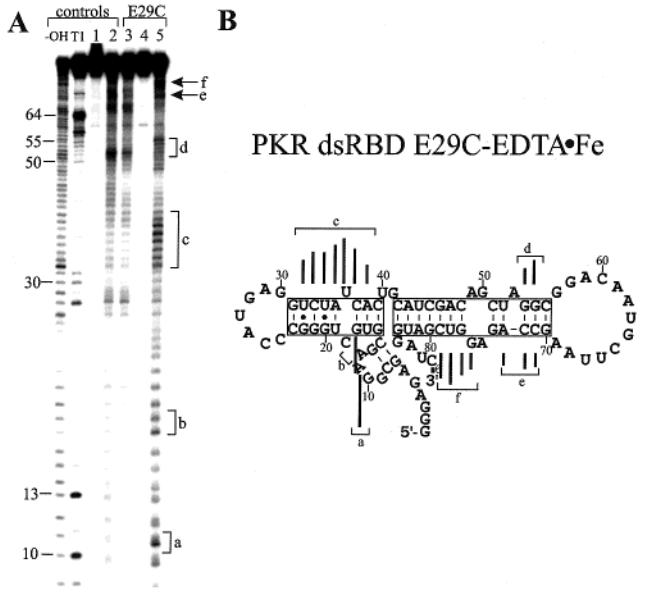

FIGURE 3: Affinity cleaving of the aptamer ligand of PKR using the EDTA·Fe modified E29C dsRBD mutant. (A) Storage phosphor autoradiogram of a 16% denaturing polyacrylamide gel separating the 5′-end labeled RNA cleavage products from the E29C PKR dsRBD mutant. -OH: alkaline ladder; T1: RNase T1 (G ladder) lane; lane 1: RNA only; lane 2: RNA in the presence of free EDTA·Fe and cleavage reagents; lane 3: unmodified E29C and RNA in the presence of free EDTA·Fe and cleavage reagents; lane 4: E29C-EDTA·Fe and RNA; lane 5: E29C-EDTA·Fe and RNA in the presence of cleavage reagents. For visualization of the location of sites labeled (e) and (f), see Figure 5B, lane 5. (B) Mapping of the major cleavage sites (identified by letters and brackets) on the aptamer's secondary structure (*33*). Boxes indicate the 5′-stem and 3′-stem structures.

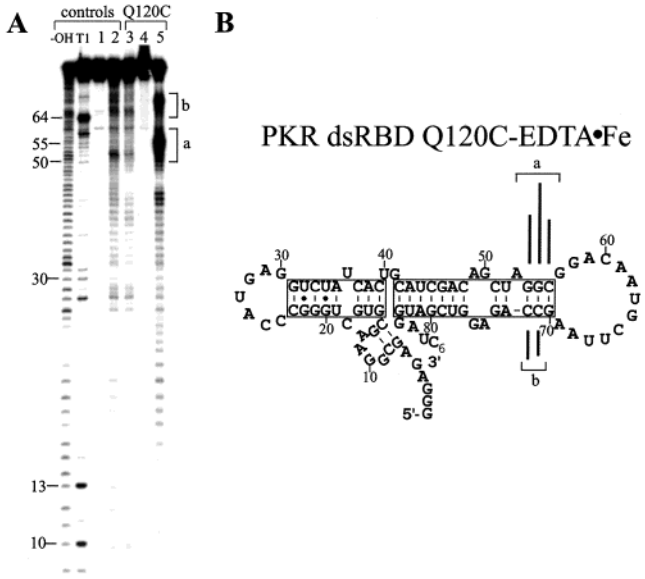

FIGURE 4: Affinity cleaving of the aptamer ligand of PKR using the EDTA·Fe modified Q120C. (A) Storage phosphor autoradiogram of a 16% denaturing polyacrylamide gel separating the 5′-end labeled RNA cleavage products generated by Q120C-EDTA·Fe. Major cleavage sites are identified with letters and brackets. Lanes are the same as outlined for Figure 3, replacing Q120C for E29C. (B) Mapping of the major cleavage sites (identified by letters and brackets) on the aptamer's secondary structure (*33*).

loops: an 8 bp 5′-stem loop with a symmetrical internal loop and a 12 bp 3′-stem loop containing two tandem G·A mismatches (Figure 3B) (*33*). With the E29C-EDTA·Fe conjugate, nucleotides in both the 5′- and 3′-stem loop structures were cleaved, suggesting more than one binding site for dsRBM I on this RNA (Figure 3, sites a−f). Cleavage with the Q120C-EDTA·Fe conjugate resulted in a single major cleavage site in the 3′-stem near the loop end (Figure 4, sites a and b). The Q120C-EDTA·Fe cleavage pattern is similar to that observed with the E29C-EDTA·Fe conjugate near the loop end of the 3′-stem (compare sites d and e, Figure 3, and sites a and b, Figure 4). These results indicate that the 3′-stem loop of the aptamer can support the binding of either dsRBM I or dsRBM II of PKR's dsRBD, whereas the 5′-stem loop only interacts with dsRBM I.

Given the observations that suggested that dsRBM I of PKR could bind the aptamer at more than one site, we wished to determine whether either of the binding sites was dependent on the binding of dsRBM II. To address this question, we prepared a dsRBD that was modified with EDTA·Fe in dsRBM I (E29C-EDTA·Fe) and harbored a mutation at a conserved RNA-binding residue in dsRBM II (K150A), creating the K150A, E29C-EDTA·Fe conjugate. The K150A mutation has been shown by others to decrease the binding affinity of PKR for RNA ligands (*34*). We also confirmed this result with the K150A, E29C-EDTA·Fe conjugate using gel mobility shift assays and various PKR ligands (data not shown). We observed a decrease in cleavage efficiency at the site in the 5′-stem and a corresponding increase in cleavage efficiency at the cleavage site near the loop end of the 3′-stem when comparing this conjugate to the E29C-EDTA·Fe protein (compare Figures 3 and 5). Thus, a mutation that hinders binding of dsRBM II decreases the extent to which the 5′-stem is bound by dsRBM I, suggesting simultaneous binding of the two motifs in this complex.

If the aptamer binds PKR in a complex involving simultaneous contact with both dsRBMs, one would predict that the cleavage efficiency observed when EDTA·Fe is covalently bound to dsRBM II would decrease when the binding of dsRBM I is disrupted by mutation. To test this hypothesis, we prepared a dsRBD that was modified with EDTA·Fe in dsRBM II (Q120C-EDTA·Fe) and was mutated at a conserved RNA-binding residue in dsRBM I (K60A), creating the K60A, Q120C-EDTA·Fe conjugate. The K60A mutation has also been shown to decrease the binding affinity of PKR for RNA ligands (*34*). We observed a substantial decrease in cleavage efficiency for this protein as compared to the Q120C-EDTA·Fe conjugate (Figure 6). Therefore, a mutation that hinders binding of dsRBM I decreases the extent to which the 3′-stem is bound by dsRBM II, again consistent with simultaneous binding of the two motifs in this complex.

Cleavage of a Kinase-Inhibiting RNA Ligand with dsRBM I and dsRBM II PKR dsRBD EDTA·Fe Conjugates. In a previous study, it was shown that the minimal structural component of the aptamer necessary for binding PKR is a 46 nt RNA comprising the 3′-stem (*33*). In contrast to the full-length aptamer, this minimal RNA is a poor activator of PKR and instead functions as a potent antagonist of kinase activation (*33*). The cleavage sites generated on this RNA by the E29C-EDTA·Fe conjugate are the same as those found near the loop end of the 3′-stem of the full-length aptamer (compare sites d and e, Figure 3, and a and b, Figure 7). Importantly, when the Q120C-EDTA·Fe conjugate was used to cleave the 46 nt minimal binding RNA, no cleavage sites

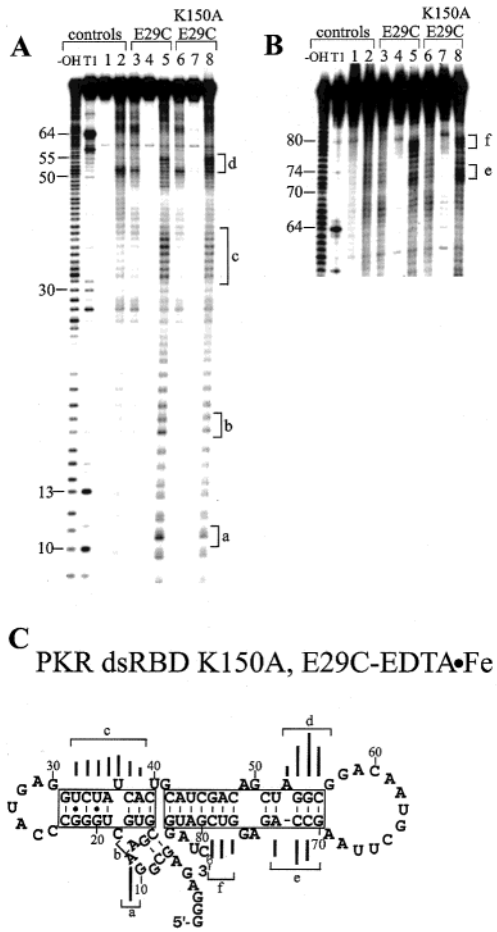

FIGURE 5: Affinity cleaving of the aptamer ligand of PKR using the E29C-EDTA·Fe conjugate harboring the K150A mutation in dsRBM II. (A) Storage phosphor autoradiogram of a 16% denaturing polyacrylamide gel separating the 5′-end labeled RNA cleavage products. -OH: alkaline ladder; T1: RNase T1 (G ladder); lane 1: RNA only; lane 2: RNA in the presence of free EDTA·Fe and cleavage reagents; lane 3: unmodified E29C and RNA in the presence of free EDTA·Fe and cleavage reagents; lane 4: E29C-EDTA·Fe and RNA; lane 5: E29C-EDTA·Fe and RNA in the presence of cleavage reagents; lane 6: unmodified K150A, E29C and RNA in the presence of free EDTA·Fe and cleavage reagents; lane 7: K150A, E29C-EDTA·Fe and RNA; lane 8: K150A, E29C-EDTA·Fe and RNA in the presence of cleavage reagents. (B) Same as in panel A with electrophoresis carried out longer to allow for visualization of sites (e) and (f). (C) Mapping of the major cleavage sites (identified by letters and brackets) on the aptamer's secondary structure by the K150A, E29C-EDTA·Fe conjugate (*33*).

were observed (Figure 7A, lane 8). This result was surprising given the observation that dsRBM II bound this RNA structure in the context of the full-length aptamer (Figure 4, sites a and b). Thus, the presence of the 5′-stem of the aptamer is necessary for dsRBM II to bind the 3′-stem.

Cleavage of the Adenovirus PKR Inhibitor VA_I RNA with dsRBM I and dsRBM II PKR dsRBD EDTA·Fe Conjugates. Previously, we used dsRBM I EDTA·Fe conjugates to locate the binding site of dsRBM I on VA_I RNA (*18*). We identified a major cleavage site for dsRBM I near the apical stem loop close to the single stranded RNA loop and a minor site in the RNA's central domain (Figure 8A, lane 5). To locate the binding site for dsRBM II on VA_I RNA, we analyzed the cleavage patterns generated by the Q120C-EDTA·Fe conjugate. The major cleavage site generated by Q120C-EDTA·Fe is in the same location as that of the E29C-EDTA·

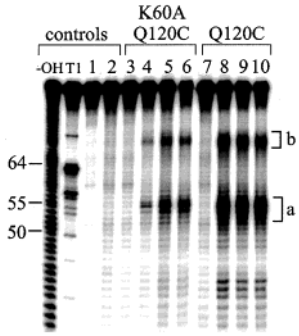

FIGURE 6: Affinity cleavage of the aptamer with K60A, Q120C-EDTA·Fe conjugate. -OH: alkaline ladder; T1: RNase T1 (G ladder); lane 1: RNA alone; lane 2: RNA in the presence of free EDTA·Fe and cleavage reagents; lane 3: 4 μM unmodified K60A, Q120C, and RNA with free EDTA·Fe and cleavage reagents; lanes 4−6: 500 nM, 1 μM and 4 μM K60A, Q120C-EDTA·Fe, and RNA with cleavage reagents, respectively; lane 7: 4 μM unmodified Q120C and RNA with free EDTA·Fe and cleavage reagents; lanes 8−10: 500 nM, 1 μM, and 4 μM Q120C-EDTA·Fe and RNA with cleavage reagents, respectively. (a) and (b) refer to cleavage sites (a) and (b) mapped in Figure 4.

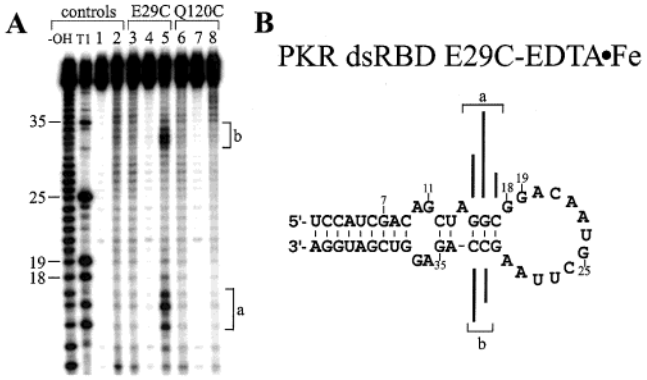

FIGURE 7: Affinity cleaving of the 46 nt minimal binding element of the aptamer RNA using the E29C-EDTA·Fe and Q120C-EDTA·Fe conjugates. (A) Storage phosphor autoradiogram of a 16% denaturing polyacrylamide gel separating the 5′-end labeled RNA cleavage products. -OH: alkaline ladder; T1: RNase T1 (G ladder); lane 1: RNA only; lane 2: RNA in the presence of free EDTA·Fe and cleavage reagents; lane 3: unmodified E29C and RNA in the presence of free EDTA·Fe and cleavage reagents; lane 4: E29C-EDTA·Fe and RNA; lane 5: E29C-EDTA·Fe and RNA in the presence cleavage reagents; lane 6: unmodified Q120C and RNA in the presence of free EDTA·Fe and cleavage reagents; lane 7: Q120C-EDTA·Fe and RNA; lane 8: Q120C-EDTA·Fe and RNA in the presence of cleavage reagents. (B) Mapping of the major cleavage sites (identified by letters and brackets) on the 46 nt RNA's secondary structure (*33*).

Fe conjugate near the end of the apical stem close to the single stranded loop (Figure 8A, lane 8). However, the minor cleavage site in the central domain observed by the E29C-EDTA·Fe conjugate is absent for Q120C-EDTA·Fe. Thus, VA_I RNA has a binding site in the apical stem that can interact with either dsRBM I or dsRBM II and a second site in the central domain that binds weakly only to dsRBM I.

DISCUSSION

Affinity Cleavage Experiments Can Identify the RNA Binding Sites of the Individual dsRBMs in a Multi-dsRBM Protein. Affinity cleavage is a widely used technique to define structural features of complexes between proteins and nucleic acids (*35*−*37*). Application of the affinity cleaving

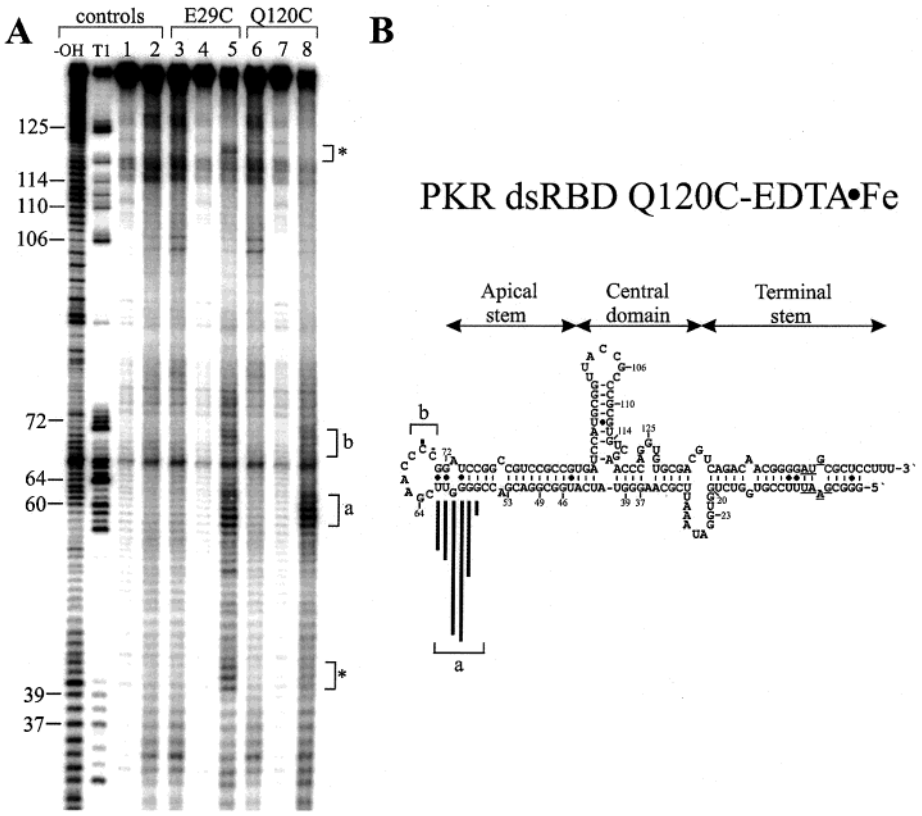

FIGURE 8: Affinity cleaving of the adenovirus VA_I RNA (a PKR kinase inhibitor) using the E29C-EDTA·Fe and Q120C-EDTA·Fe conjugates. (A) Storage phosphor autoradiogram of a 12% denaturing polyacrylamide gel separating the 5′-end labeled RNA cleavage products from PKR dsRBD conjugates. -OH: alkaline ladder; T1: RNase T1 (G ladder); lane 1: RNA only; lane 2: RNA in the presence of free EDTA·Fe and cleavage reagents; lane 3: unmodified E29C and RNA in the presence of free EDTA·Fe and cleavage reagents; lane 4: E29C-EDTA·Fe and RNA; lane 5: E29C-EDTA·Fe and RNA in the presence of cleavage reagents; lane 6: unmodified Q120C and RNA in the presence of free EDTA·Fe and cleavage reagents; lane 7: Q120C-EDTA·Fe and RNA; lane 8: Q120C-EDTA·Fe and RNA in the presence of cleavage reagents. (B) Mapping of the major cleavage sites (identified by letters and brackets) on the secondary structure model of the adenovirus VA_I RNA. The weak cleavage indicated by an asterisk corresponds to a site in the central domain of VA_I RNA and is observed only with E29C-EDTA·Fe (*18*).

technique is particularly appropriate in the study of PKR due to PKR's ability to bind many different RNAs with simple and complex structures (*2*, *3*, *27*, *38*, *39*). Furthermore, PKR's dsRBD is composed of two copies of the dsRBM and the precise role of the individual dsRBMs in PKR's binding mechanism is poorly understood. In this study, we incorporated EDTA·Fe at sites in either dsRBM I or dsRBM II and analyzed cleavage patterns generated on kinase-activating and kinase-inhibiting RNAs. These experiments have provided insight into the organization of PKR's dsRBD on these RNAs. With all of the RNAs studied, we observed localized cleavage patterns generated by the dsRBD EDTA·Fe conjugates, indicating a limited number of binding sites for PKR's dsRBMs.

In the case of TAR RNA, identification of binding sites for dsRBM I and dsRBM II allows us to speculate on the structure of the TAR RNA·PKR dsRBD complex with a molecular model based on the cleavage data and the crystal structure of Xlrbpa bound to duplex RNA (Figure 9). The structure of an RNA corresponding to 29 nt of the loop end of TAR RNA has been solved by NMR (*29*). To this structure, we appended a duplex extension to model the full-length 59 nt TAR RNA. The nucleotides cleaved by the various EDTA·Fe conjugates were mapped onto this structural model for TAR, and the two dsRBMs were docked onto the RNA. This docking was guided by maintaining proximity

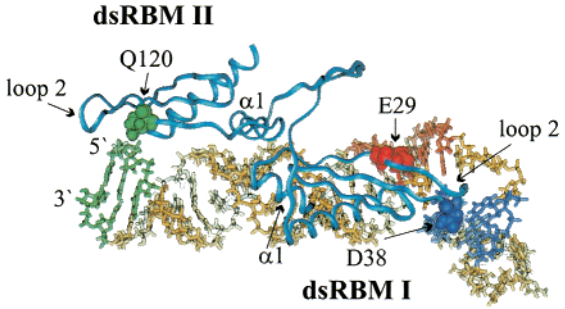

FIGURE 9: Model of the complex formed by the binding of PKR's dsRBD to TAR RNA based on the observed cleavage data. EDTA·Fe-modified amino acid positions with their cleaved nucleotides are highlighted in color.

between the three clusters of surface amino acids observed to be in contact with the RNA in the Xlrbpa·RNA structure and their corresponding binding site on the RNA (region I: minor groove, region II: minor groove, and region III: major groove) (*16*). In addition, the dsRBMs were placed on the RNA such that the amino acid position modified with EDTA·Fe is near nucleotides cleaved by the corresponding EDTA·Fe conjugate. Figure 9 shows the resulting molecular model wherein dsRBM I is located near the loop end of TAR and dsRBM II is bound in the opposite orientation at the other end of the TAR molecule. This places dsRBM II on a face of the RNA approximately 90° rotated from that of the

dsRBM I binding site. This model predicts close contact between various amino acid residues in the protein and nucleotides in the RNA and, thus, provides a basis for future experiments designed to probe the binding mechanism. Interestingly, this model suggests that TAR may have a duplex that is close to the minimum length necessary to support simultaneous binding of both dsRBM I and dsRBM II.

Some RNA Binding Sites Interact only with One dsRBM, while Others Can Bind either dsRBM I or dsRBM II. An important observation made in this work is that some, but not all, binding sites for PKR's dsRBMs are selective for either dsRBM I or dsRBM II. For instance, the 5′-stem loop of the aptamer binds only dsRBM I (Figures 3 and 4). Also, the loop end of TAR binds only dsRBM I, whereas the duplex formed at TAR's 5′-end binds only dsRBM II (Figure 2). The binding site on the minimal binding element of the aptamer is occupied only by dsRBM I (Figure 7). The binding site in the central domain of VA_I RNA is apparently only bound by dsRBM I (Figure 8). These examples stand in contrast to the binding site formed by the 3′-stem of the aptamer, which can be bound by either dsRBM I or dsRBM II (Figures 3 and 4). This promiscuity in binding is also observed for the apical stem structure of VA_I RNA (Figure 8). Inspection of the sequences of "selective" RNA binding sites and "promiscuous" binding sites offers little insight into why they may bind with different selectivities. Of the RNAs studied here, TAR RNA is unique as it has one selective binding site for dsRBM I and one selective binding site for dsRBM II, suggesting that TAR could form a single complex in solution with the two dsRBMs bound simultaneously. Since TAR RNA does not have promiscuous binding sites, it is an excellent candidate for future high-resolution structural analysis of the complex formed with the PKR dsRBD.

EDTA·Fe Modification Coupled with Site-Directed Mutagenesis Can Be Used to Assess the Extent of Cooperativity between dsRBMs in the Binding of a multi-dsRBM Protein. In the analysis of the binding of dsRBD EDTA·Fe conjugates to the aptamer, it became apparent that this RNA had at least two binding sites for dsRBM I. This was unexpected given that gel mobility shift experiments with this RNA and PKR's dsRBD show only one band for the protein−RNA complex (*26*). To determine if dsRBM II contributed to the binding at either of the dsRBM I binding sites, we used a protein that carried EDTA·Fe on dsRBM I and a mutation in dsRBM II that hindered its binding to the RNA (K150A, E29C-EDTA·Fe conjugate). Experiments with this protein revealed that binding of dsRBM I to the 5′-stem loop site was dependent on the binding of dsRBM II. Furthermore, cleavage experiments were carried out with the K60A, Q120C-EDTA·Fe protein, where the RNA affinity of dsRBM I is decreased by the K60A mutation and the binding of dsRBM II is monitored by EDTA·Fe cleavage. The lower cleavage efficiency observed for this protein relative to the conjugate with a wild-type dsRBM I support the conclusion that the binding of dsRBM II to the 3′-stem requires the binding of dsRBM I. Since dsRBM I binds the 5′-stem and the binding of dsRBM II contributes to this interaction, we conclude that PKR's dsRBD binds the full length aptamer in a complex with dsRBM I bound in the 5′-stem and dsRBM II in the 3′-stem (Figure 10, complex 1). We envision the

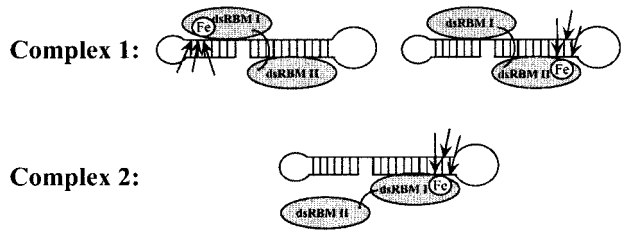

FIGURE 10: Schematic of complexes formed by the binding of the dsRBD of PKR to the aptamer. Complex 1 is formed by the simultaneous binding of dsRBM I to the 5′-stem and dsRBM II to the 3′-stem. Cleavage products are observed for this complex with either dsRBM I or dsRBM II modified with EDTA·Fe. Complex 2 is formed by the binding of dsRBM I to the 3′-stem with dsRBM II not contributing to the binding affinity. Cleavage products are observed for this complex only when dsRBM I is EDTA·Fe modified.

binding site of dsRBM I in this complex being composed of duplex arising from the coaxial stacking of the 5′-stem and the 3′-stem. This would generate an RNA structure with a duplex region similar in length to that found in TAR RNA (aptamer: 23 bp vs TAR: 24 bp) and thus, could support the simultaneous binding of dsRBM I and dsRBM II as depicted in Figure 9 for TAR. Coaxial stacking of the 5′- and 3′-stems also explains the observation of the cleavage site labeled (f) in Figures 3 and 5, as nucleotides at this location would reside on the same face of the duplex as those of the major site of cleavage in the 5′-stem (Figures 3 and 5, site c). Therefore, the nucleotides in site (f) could be cleaved by the EDTA·Fe complex responsible for site (c). This cleavage site is only observed with the E29C-EDTA·Fe conjugate and only when the 5′-stem is present in the RNA structure (see Figure 7).

However, in contrast to TAR RNA, the aptamer can also support an additional complex with PKR (Figure 10, complex 2). In this complex, dsRBM II is apparently not in contact with the RNA as decreasing its binding affinity with the K150A mutation lead to an *increase* in the dsRBM I-induced cleavage in the 3′-stem. Interestingly, it is this binding mode that is maintained by the minimal binding element of the aptamer (Figure 7). Thus, these experiments revealed two ways in which PKR's dsRBD binds the aptamer RNA, one of which involves simultaneous binding of both PKR's dsRBMs and one that involves the independent binding of dsRBM I (Figure 10, complexes 1 and 2, respectively). This demonstration of the combination of affinity cleaving to follow the binding of one motif and site-directed mutagenesis to alter the binding affinity of another motif may prove useful in the future analysis of cooperativity in the binding of dsRBMs for other multi-dsRBM proteins.

Kinase Activating RNAs Studied here Have Binding Sites that Could Support the Simultaneous Binding of dsRBM I and dsRBM II of PKR. Part of the motivation for this work was to determine if differences could be observed in the organization of PKR's dsRBD on RNA ligands that differed in their ability to activate PKR's kinase domain. Results of past studies have suggested a requirement for the simultaneous binding of both dsRBMs on an RNA ligand for kinase activation to occur (*40*). For example, the dependence of RNA duplex length in PKR's activation could arise from the necessity of the simultaneous binding of both dsRBMs of PKR's dsRBD (*2*). NMR experiments of PKR's dsRBD suggested that dsRBM II, but not dsRBM I, interacts with

the kinase domain (*25*). The authors suggest that dsRBM II may function as a negative regulator of PKR's kinase activity via contact with the kinase domain when it is not bound to RNA. This proposal is consistent with the observation that when PKR's kinase domain is expressed independently, free of the dsRBD, it is a constitutively active protein kinase (*24*). The simultaneous binding of dsRBM I and dsRBM II to RNA is then believed to release the kinase domain and lead to activation. PKR is also observed to be activated at low concentrations of duplex RNA, whereas at high concentrations, these RNAs function as inhibitors of the kinase (*22*). These results could also be explained by the requirement for simultaneous contact of both of PKR's dsRBMs to a single RNA molecule, which would occur at low RNA:protein ratios. At high concentrations of RNA, each dsRBM could bind a different RNA molecule leading to kinase inhibition.

Given the above observations, one might then predict that an activating RNA ligand would have binding sites that can support the simultaneous binding of both dsRBMs of PKR. The cleavage results observed in this study are consistent with that idea. The cleavage sites observed for dsRBM I and dsRBM II with the two activating RNA ligands (TAR RNA and the aptamer) signify two separate binding sites for the motifs. For example, TAR RNA's structure creates two separate binding sites that can bind to dsRBM I or dsRBM II, respectively. In our model of the TAR·dsRBD complex, loop 2 of dsRBM II does not contact the RNA thus giving this motif only two of the three regions of RNA contact found in the Xlrbpa crystal structure. This fact may have contributed to the past difficulty in assessing the ability of TAR to function as a PKR activator (*32*, *41*). The aptamer also has different binding sites for the two dsRBMs. Indeed, results of experiments with mutant proteins deficient in binding via dsRBM I or dsRBM II and a truncated form of the RNA indicate that the aptamer can bind both motifs simultaneously. The minimal binding element from this aptamer binds only dsRBM I and is not an activator of PKR, but rather functions as an inhibitor. Thus, one mechanism by which an RNA may function as an inhibitor is to provide enough duplex structure to bind only to dsRBM I.

Given the data that suggest dsRBM II functions as an autoinhibitory domain, one might predict that an RNA molecule that binds dsRBM II would function as a PKR activator. However, the kinase inhibiting VA_I RNA from adenovirus can support the binding of dsRBM II in its apical stem structure (Figure 8, lane 8). Therefore, the ability to bind to dsRBM II does not necessarily distinguish kinase-activating from kinase- inhibiting RNAs. We believe the simultaneous binding of an RNA molecule to both dsRBMs leads to the conformational change necessary to activate the enzyme. For this to occur with VA_I RNA, dsRBM II would bind the apical stem, leaving dsRBM I to bind in its central domain binding site. However, the inefficient cleavage observed with the dsRBM I conjugates in the central domain of VA_I RNA suggests this is an inferior binding site for this motif. It has been reported that the central domain structure of VA_I RNA is important for PKR inhibition (*42*). It may be the case that the unique structure of the central domain allows for some interaction with dsRBM I, but this interaction is insufficient to promote the activating conformational change in the kinase domain.

In summary, we have shown that EDTA·Fe affinity cleavage can be used to identify binding sites for the individual dsRBMs in PKR's dsRBD on various RNA ligands. Some RNA binding sites interact only with a single dsRBM, while others can bind either dsRBM I or dsRBM II. Importantly, the RNAs studied here that function as activators of PKR have binding sites that could support the simultaneous binding of dsRBM I and dsRBM II. These results support the hypothesis that simultaneous binding of both dsRBMs of PKR occurs during RNA-mediated activation.

REFERENCES

1. Kaufman, R. (1999) *Proc. Natl. Acad. Sci. U.S.A. 96*, 11693−11695.
2. Manche, L., Green, S. R., Schmedt, C., and Mathews, M. B. (1992) *Mol. Cell. Biol. 12*, 5238−5248.
3. Circle, D. A., Neel, O. D., Robertson, H. D., Clarke, P. A., and Mathews, M. B. (1997) *RNA 3*, 438−448.
4. Williams, B. R. G. (1999) *Oncogene 18*, 6112−6120.
5. DeHaro, C., Mendez, R., and Santoyo, J. (1996) *FASEB 10*, 1378−1387.
6. Kitajewski, J., Schneider, R. J., Safer, B., Munemitsu, S. M., Samuel, C. E., Thimmappaya, B., and Shenk, T. (1986) *Cell 45*, 195−200.
7. Clarke, P. A., Sharp, N. A., and Clemens, M. J. (1990) *Eur. J. Biochem. 193*, 635−641.
8. Meurs, E., Chong, K., Galabru, J., Thomas, N. S. B., Kerr, I. M., Williams, B. R. G., and Hovanessian, A. G. (1990) *Cell 62*, 379−390.
9. Fierro-Monti, I., and Mathews, M. B. (2000) *Trends Biochem. Sci. 25*, 241−246.
10. Bass, B. L., Nishikura, K., Keller, W., Seeburg, P. H., Emeson, R. B., O'Connell, M. A., Samuel, C. E., and Herbert, A. (1997) *RNA 3*, 947−949.
11. Bycroft, M., Gruenert, S., Murzin, A. G., and Proctor, M. (1995) *EMBO J. 14*, 3563−3571.
12. Kharrat, A., Macias, M. J., Gibson, T. J., and Nilges, M. (1995) *EMBO J. 14*, 3572−3584.
13. Langland, J. O., Kao, P. N., and Jacobs, B. L. (1999) *Biochemistry 38*, 6361−6368.
14. Jaramillo, M. L., Abraham, N., and Bell, J. C. (1995) *Cancer Invest. 13*, 327−338.
15. Nanduri, S., Carpick, B. W., Yang, Y., Williams, B. R. G., and Qin, J. (1998) *EMBO J. 17*, 5458−5465.
16. Ryter, J. M., and Schultz, S. C. (1998) *EMBO J. 17*, 7505−7513.
17. Ramos, A., Grunert, S., Adams, J., Micklem, D. R., Proctor, M. R., Freund, S., Bycroft, M., St. Johnston, D., and Varani, G. (2000) *EMBO J. 19*, 997−1009.
18. Spanggord, R. J., and Beal, P. A. (2001) *Biochemistry 40*, 4272−4280.
19. Tian, B., and Mathews, M. B. (2001) *J. Biol. Chem. 276*, 9936−9944.
20. Bevilacqua, P. C., and Cech, T. R. (1996) *Biochemistry 35*, 9983−9994.
21. Green, S. R., and Mathews, M. B. (1992) *Genes Dev. 6*, 2478−2490.
22. Galabru, J., and Hovanessian, A. (1987) *J. Biol. Chem. 262*, 15538−15544.
23. Carpick, B. W., Graziano, V., Schneider, D., Maitra, R. K., Lee, X., and Williams, B. R. G. (1997) *J. Biol. Chem. 272*, 9510−9516.
24. Wu, S., and Kaufman, R. J. (1996) *J. Biol. Chem. 271*, 1756−1763.
25. Nanduri, S., Rahman, F., Williams, B. R. G., and Qin, J. (2000) *EMBO J. 19*, 5567−5574.
26. Spanggord, R. J., and Beal, P. A. (2000) *Nucleic Acids Res. 28*, 1899−1905.

27. Clarke, P. A., and Mathews, M. B. (1995) *RNA 1*, 7−20.
28. Milligan, J. F., Groebe, D. R., Witherell, G. W., and Uhlenbeck, O. C. (1987) *Nucleic Acids Res. 15*, 8783−8798.
29. Aboul-ela, F., Karn, J., and Varani, G. (1996) *Nucleic Acids Res. 24*, 3974−3981.
30. Muesing, M. A., Smith, D. H., and Capon, D. J. (1987) *Cell 48*, 691−701.
31. Edery, I., Petryshyn, R., and Sonenberg, N. (1989) *Cell 56*, 303−312.
32. Maitra, R. K., McMillan, N. A. J., Desai, S., McSwiggen, J., Hovanessian, A. G., Sen, G., Williams, B. R. G., and Silverman, R. H. (1994) *Virology 204*, 823−827.
33. Bevilacqua, P. C., George, C. X., Samuel, C. E., and Cech, T. R. (1998) *Biochemistry 37*, 6303−6316.
34. Patel, R. C., Stanton, P. and Sen, G. C. (1996) *J. Biol. Chem. 271*, 25657−25663.
35. Pendergrast, P. S., Ebright, Y. W., and Ebright, R. H. (1994) *Science 265*, 959−962.
36. Oakley, M. G., and Dervan, P. B. (1990) *Science 248*, 847−850.
37. Heilek, G. M., and Noller, H. F. (1996) *Science 272*, 1659−1662.
38. Clarke, P. A., Schwemmle, M., Schickinger, J., Hilse, K., and Clemens, M. J. (1991) *Nucleic Acids Res. 19*, 243−248.
39. Tian, B., White, R. J., Xia, T., Welle, S., Turner, D. H., Mathews, M. B., and Thornton, C. A. (2000) *RNA 6*, 79−87.
40. Robertson, H. D., and Mathews, M. B. (1996) *Biochimie 78*, 909−914.
41. Gunnery, S. G., Rice, A. P., Robertson, H. D., and Mathews, M. B. (1990) *Proc. Natl. Acad. Sci. U.S.A. 87*, 8687−8691.
42. Ma, Y., and Mathews, M. B. (1996) *RNA 2*, 937−955.

BI0120594